

Solving Inverse Problems in Steady State Navier-Stokes Equations using Deep Neural Networks

Tiffany Fan,¹ Kailai Xu,¹ Jay Pathak,² Eric Darve^{1,3}

¹Institute for Computational and Mathematical Engineering, Stanford University, Stanford, CA 94305, USA; {tiffan, kailaix, darve}@stanford.edu

² ANSYS, Inc, San Jose, CA 95134, USA; jay.pathak@ansys.com

³ Mechanical Engineering, Stanford University, Stanford, CA 94305, USA

Abstract

Inverse problems in fluid dynamics are ubiquitous in science and engineering, with applications ranging from electronic cooling system design to ocean modeling. We propose a general and robust approach for solving inverse problems for the steady state Navier-Stokes equations by combining deep neural networks and numerical PDE schemes. Our approach expresses numerical simulation as a computational graph with differentiable operators. We then solve inverse problems by constrained optimization, using gradients calculated from the computational graph with reverse-mode automatic differentiation. This technique enables us to model unknown physical properties using deep neural networks and embed them into the PDE model. Specifically, we express the Newton’s iteration to solve the highly nonlinear Navier-Stokes equations as a computational graph. We demonstrate the effectiveness of our method by computing spatially-varying viscosity and conductivity fields with deep neural networks (DNNs) and training DNNs using partial observations of velocity fields. We show that DNNs are capable of modeling complex spatially-varying physical field with sparse and noisy data. We implement our method using ADCME, a library for solving inverse modeling problems in scientific computing using automatic differentiation.

1 Introduction

Fluid dynamics has been used for a wide variety of applications in chip design (Fedorov and Viskanta 2000), earth exploration (Li et al. 2020), weather forecasting (Zajczkowski, Haupt, and Schmehl 2011), and so on. However, quantifying fluid properties of the governing equations, which are essential for predictive modeling, can be expensive or impossible to determine from experiments directly (Cotter et al. 2009). This challenge leads us to leverage indirect data, which are not direct observations of fluid properties but carry relevant information via governing equations. Making sense of the indirect data is challenging, because we need to consider the relationship among governing equations, data, and fluid properties as a whole.

The governing equations considered in this paper are the steady state Navier-Stokes equations for incompressible

flow

$$(\mathbf{u} \cdot \nabla)\mathbf{u} = -\frac{1}{\rho}\nabla p + \nabla \cdot (\nu \nabla \mathbf{u}) + \mathbf{g} \quad (1)$$

with $\nabla \cdot \mathbf{u} = 0$, and where ρ is the fluid density, \mathbf{u} is the vector of flow velocity, p is the pressure, ν is the kinematic viscosity field, and \mathbf{g} is the vector of body accelerations. The system is highly nonlinear, and thus the numerical simulation requires Newton’s iterations.

One example of inverse problem is to estimate a spatially-varying $\nu(\mathbf{x})$ from partially observed data \mathbf{u} . Here the observation is considered “indirect” because ν is not directly measured. Additionally, because we only have a limited amount of observations, the inverse problem may be ill-posed (there are multiple ν that produce the same observations). Here, we propose using a deep neural network (DNN) (Goodfellow et al. 2016) to approximate the quantity of interest, such as ν , as a regularizer. The inputs to the DNN are coordinates and the outputs are values of ν at the corresponding locations.

Our major contribution is to propose a general approach to couple DNNs and an iterative PDE solver for the steady-state Navier-Stokes equations. The basic idea is to express both DNNs and PDE solvers with a computational graph. Therefore, once we implement the forward simulation, the gradients can be easily extracted from the computational graph using reverse-mode automatic differentiation (Margossian 2019; Baydin et al. 2017). The major challenge is that we need to design and implement a collection of numerical simulation operations with gradient back-propagation capability. We demonstrate our method on three problems, and in the last two, the Navier-Stokes equations are coupled with a heat equation and a transport equation.

2 Methodology

2.1 Deep Neural Networks for Inverse Problems

When the fluid properties are complex spatially-varying functions, the resulting constrained optimization problems have infinite-dimensional feasible spaces. Solving such optimization problems with traditional basis functions, such as piecewise linear basis functions and radial basis functions, is challenging. Thus, we use deep neural networks (DNNs) to approximate the fluid properties in order to ensure the flexibility of the approximation. The inputs of the DNNs

are spatial coordinates of a given point in the domain, and the output is the predicted model parameter at that point. DNNs are high dimensional nonlinear functions of the inputs and have demonstrated abilities to approximate complex unknown functions. In addition, with certain choices of activation functions, such as tanh and sigmoid functions, the DNNs are continuous functions of the inputs. The inherent regularity effect of the DNNs results in more accurate approximations to the true fluid properties in many physical scenarios.

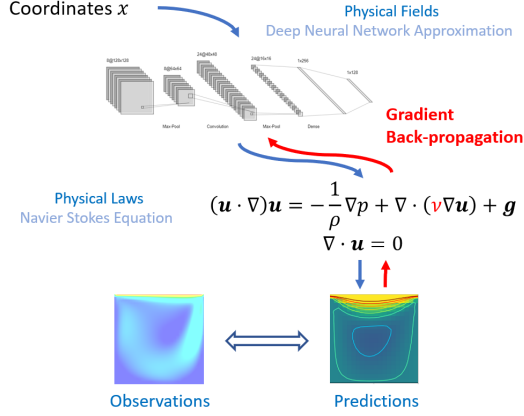


Figure 1: Schematic diagram of using deep neural networks to approximate spatially-varying physical fields. Note that only $\nu(\mathbf{x})$ is approximated by a neural network, and the solution u is still defined on the discretized grid points. Deep neural networks are coupled with PDEs and gradients are back-propagated through both PDE solvers and DNNs.

2.2 Constrained Optimization for Inverse Problems

In the abstract, we formulate an inverse problem in the context of constrained optimization

$$\begin{aligned} \min_{\theta} L(u) \quad (&u \text{ is indirectly a function of } \theta) \\ \text{s.t. } F(u, \theta) &= 0 \end{aligned}$$

where (i) the variables θ are model parameters or neural network weights and biases; (ii) the objective function L for minimization is a loss function, which measures the discrepancy between the observation and the prediction u generated by forward computation; (iii) the constraints F are the governing equations derived from physical laws. By solving the constrained minimization problem, we obtain the optimal values for the variables, which provide the optimal approximation to the physical properties of interest.

In our method, the constrained optimization problem is converted to an unconstrained one by first solving for u using the physical constraint $F(u, \theta) = 0$, i.e., $u = G(\theta)$. Then we solve the unconstrained optimization problem

$$\min_{\theta} L(G(\theta))$$

2.3 Expressing Numerical Simulation using a Computational Graph

In order to solve an inverse problem in the unconstrained optimization formulation, we use a gradient-based optimization algorithm. The challenge here is to compute the gradient $\nabla_{\theta} L(G(\theta))$. We construct the numerical simulator as a computational graph with differentiable operations, as shown in Figure 2. In each iteration of the optimization algorithm, we first perform forward computation to solve the governing equations based on the current DNN weights and biases, and evaluate the loss function by comparing the computed physical quantities with the observed data. Then, we compute the gradients using reverse-mode automatic differentiation. Finally, we update the DNN weights and biases according to the optimization algorithm, using the numerical gradients. In the numerical examples, we use the L-BFGS-B optimization algorithm (Liu and Nocedal 1989), which performs a line search in the direction of gradient descent in every iteration.

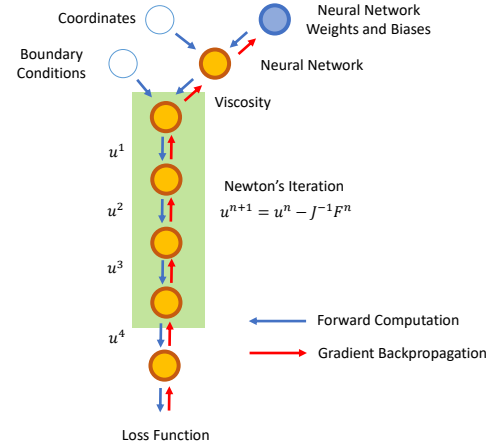


Figure 2: Expressing numerical simulation as a computational graph. The orange nodes denote numerical operators. The solid blue node denotes variables that are updated during the process of optimization. The empty blue node denotes parameters that are fixed in this process.

2.4 Physics Constrained Learning for the Nonlinear Fluid Solver

Eq. (1) describes the motion of viscous flow formed by a fluid material. The corresponding weak form is (Rannacher 2000)

$$\begin{aligned} \left(u \frac{\partial u}{\partial x}, \delta u' \right) + \left(v \frac{\partial u}{\partial y}, \delta u' \right) \\ = \frac{1}{\rho} \left(p, \frac{\partial \delta u'}{\partial x} \right) - (\nabla u, \nu \nabla \delta u') + (f, \delta u') \end{aligned} \quad (2)$$

$$\begin{aligned} \left(u \frac{\partial v}{\partial x}, \delta v' \right) + \left(v \frac{\partial v}{\partial y}, \delta v' \right) \\ = \frac{1}{\rho} \left(p, \frac{\partial \delta v'}{\partial y} \right) - \nu (\nabla v, \nabla \delta v') + (g, \delta v') \end{aligned} \quad (3)$$

$$\left(\frac{\partial u}{\partial x}, \delta p' \right) + \left(\frac{\partial v}{\partial y}, \delta p' \right) = 0 \quad (4)$$

Here $\mathbf{u} = (u, v)$ and p are the trial functions, $\delta u'$, $\delta v'$ and $\delta p'$ are test functions; ν is the viscosity coefficient. Note the system (Eqns. (2) to (4)) is highly nonlinear. To solve the nonlinear system, we use Taylor’s expansion to linearize the equation, then use the Newton’s iterative method (Beam and Bailey 1988).

The basic idea is to express all the computation using differentiable operators and construct a computational graph. For example, $(\nabla u, \nu \nabla \delta u')$ corresponds to a sparse block in the Jacobian matrix. We need an operator that consumes ν and outputs the sparse block. The operator should also be able to back-propagate downstream gradients, i.e., computing $\frac{\partial L(a(\nu))}{\partial \nu}$ given $\frac{\partial L(a)}{\partial a}$. Here L is a scalar loss function and a are entries in the sparse block. We refer readers to (Xu and Darve 2020) on how to derive and implement such operators using physics constrained learning (PCL).

Note that the numerical solver for the Navier-Stokes equation is iterative. However, we found that the solver typically converges very fast (within 5 iterations) to a very small residual. Therefore, in the gradient back-propagation, we can differentiate through each iteration in the forward computation, which is shown in Fig. 1.

3 Numerical Experiments

In this section, we demonstrate our method using three examples, and in the last two we consider a coupled system of Navier-Stokes equations and heat equations/transport equations. In all the following examples, DNNs have the same architecture: 3 layers, 20 neurons per layer, and \tanh activation functions. All the numerical examples are implemented using ADCME.jl.

3.1 Learning Spatially-varying Viscosity in Steady State Navier-Stokes Equations

We evaluate our method on a lid-driven cavity flow problem. The governing equation is given by Eq. (1), with the viscosity coefficient

$$\nu(x, y) = 1 + 6x^2 + \frac{x}{1 + 2y^2}$$

We approximate ν using a DNN, $\nu_\theta(x, y)$, where θ is the weight and biases.

In this example, the observations are \mathbf{u} at grid points, and the pressure is unknown. The observations are simulated on a grid of size 21×21 , with constant density $\rho = 1$ and velocity $u = 1$ along $y = 0$. We use the velocity data to train the DNN ν_θ . The estimated viscosity is shown in Fig. 3.

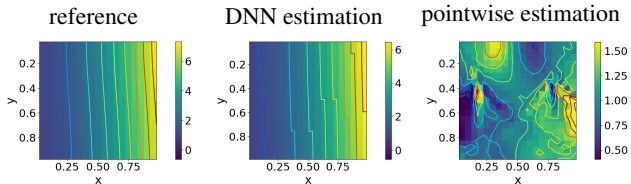


Figure 3: A comparison of estimations by the DNN and by pointwise values. The DNN provides a continuous and more accurate approximation to the reference viscosity function.

Then, we plug the estimated ν into Eq. (1) and solve for u, v , and p . The result is shown in Fig. 4. We can see that the predictions are quite close to the reference.

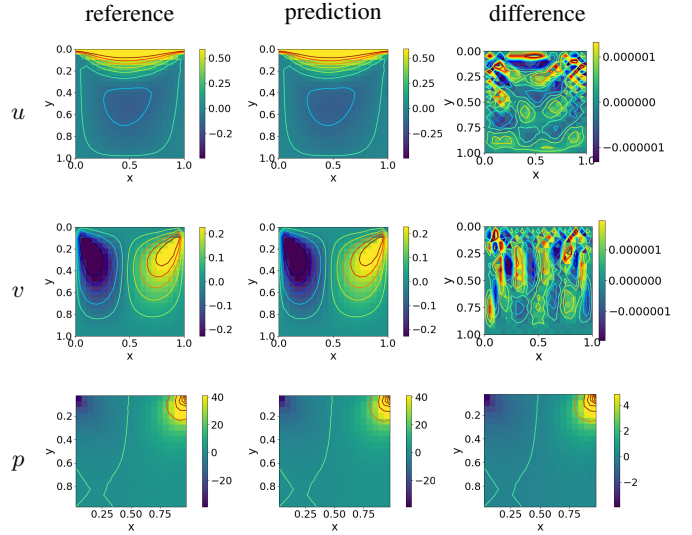


Figure 4: The reference velocity field and pressure, predictions from the DNN, and the corresponding error. We note that the loss function only contains the velocity data. However, benefiting from the physical constraints imposed by the numerical schemes, the DNN provides an accurate prediction to the pressure as well.

We also compare the DNN results with those of pointwise estimation, where we optimize the values at each grid point instead of using a function approximator (e.g., DNN). In Fig. 3, We can see that DNNs provide regularization that produces a smooth profile of the viscosity field, with relative mean square error 1.26%. The pointwise estimation is far off from the exact ν , with relative mean square error 59.14%, despite producing \mathbf{u} predictions similar to the observations.

Fig. 5 shows the convergence plot of the loss functions for both DNN and pointwise estimation. The pointwise estimation achieves smaller loss because the viscosity representation of the pointwise estimation is less constrained than that of the DNN. However, the DNN provides better viscosity estimation due to its regularization effect.

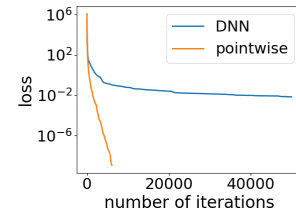


Figure 5: The convergence of loss functions using DNN and pointwise estimation.

Further evidence is shown in Fig. 6, where we compare the error in the pressure predictions provided by DNN and pointwise estimation. The pressure profile is unobserved by both methods. Thus, for the pointwise estimation, large error

in pressure prediction and small training loss indicate potential overfitting of the observed data. On the other hand, the DNN estimation produces an accurate estimation of the real pressure field without observing the pressure profile, thanks to the regularization effect of DNNs.

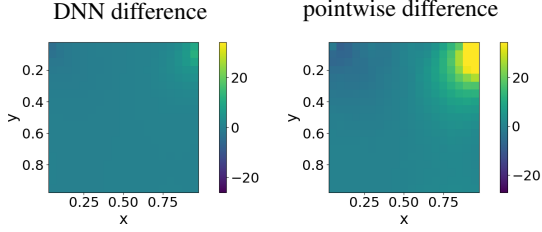


Figure 6: The error of pressure predictions from DNN and pointwise estimation.

3.2 Learning Spatially-varying Conductivity in Conjugate Heat Transfer Navier-Stokes Equations

In this example, we consider the coupled system Eq. (1) and the energy equation:

$$\rho C_p \mathbf{u} \cdot \nabla T = \nabla \cdot (k \nabla T) + Q \quad (5)$$

where C_p is the specific heat capacity, T is the temperature, k is the conductivity, and Q is the power source. The problem arises from conjugate heat transfer analysis (Wang, Wang, and Li 2007), where the heat transfers between solid and fluid domains by exchanging thermal energy at the interfaces between them.

We simulate the velocity, pressure and temperature data via forward computation with $\rho = 1$, $C_p = 1$, and

$$k(x, y) = 1 + x^2 + \frac{x}{1 + y^2}$$

The observations are the velocity and temperature data at 40 randomly sampled points from the 21×21 grid. The pressure is assumed to be unknown. Fig.7 shows that the DNN produces an accurate approximation for conductivity from the limited data.

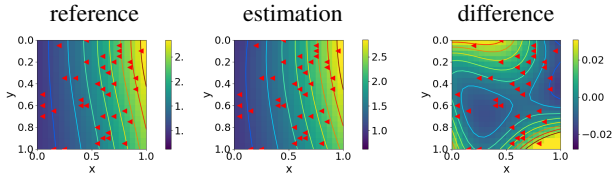


Figure 7: The reference conductivity, the estimated conductivity by the DNN, and the estimation error after 100 optimization steps. The 40 randomly sampled grid points, where velocity and temperature data are observed, are labeled with red triangles.

We also investigate the robustness of our method. To this end, we add a multiplicative noise sampled uniformly from

$[-\epsilon, \epsilon]$. The results after 100 optimization steps are shown in Fig. 8. We see that the error increases as the noise level increases, but the ν estimation is still very accurate. This implies that our approach is quite robust to noise.

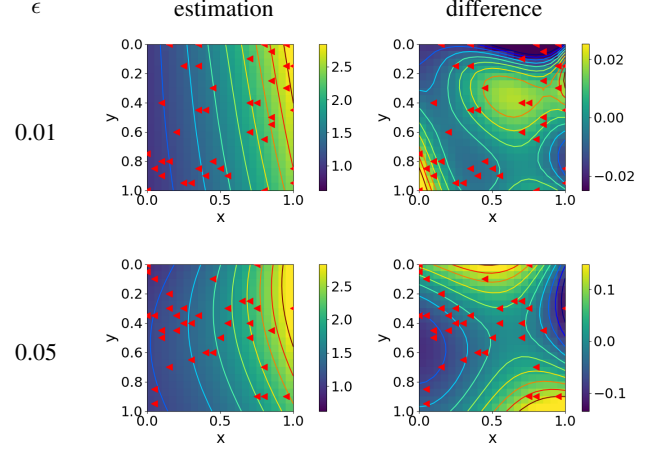


Figure 8: The estimation of viscosity functions from sparse observation of noisy data and the corresponding error. The 40 randomly sampled grid points, where velocity and temperature data are observed, are labeled with red triangles.

3.3 Learning Spatially-varying Viscosity in Passive Transport Equations

We consider an application of our method to estimate the viscosity coefficient from observations of passive particle. In this example, we only partially observe the trajectories of passive particle, whose governing equations for velocities are as follows

$$\begin{aligned} \frac{\partial w_1}{\partial t} &= \kappa_1(u - w_1) + q_1 \\ \frac{\partial w_2}{\partial t} &= \kappa_2(v - w_2) + q_2 \end{aligned}$$

Here (u, v) are the velocity field from Eq. (1), and (w_1, w_2) are the passive particle velocities. We assume that (w_1, w_2) are partially observed, and we want to estimate a space varying viscosity coefficient ν . This problem appears in many applications. For example, in the modeling of nasal drug delivery (Basu et al. 2020), (u, v) represents the airflow velocity field and (w_1, w_2) represents the droplet velocity field. The observations are simulated with $\rho = 1$, $\kappa_1 = 1$, $\kappa_2 = 1$, and kinematic viscosity

$$\nu(x, y) = 0.01 + \frac{0.01}{1 + x^2}$$

In this example, we consider a layered model for ν : the viscosity coefficient only depends on the x coordinate. We found that the current data are not sufficient to estimate ν that depends on both x and y . The reference viscosity, the estimation and error after 100 optimization steps are summarized in Fig. 9.

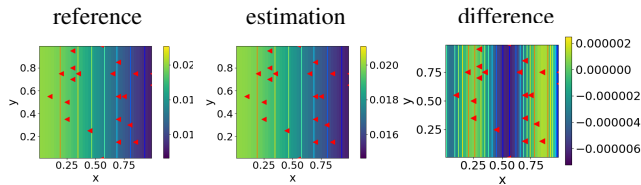


Figure 9: The reference viscosity, the estimated viscosity by the DNN, and the estimation error. The 22 randomly sampled grid points, where velocity and temperature data are observed, are labeled with red triangles.

4 Discussion

Despite the generality of our approach, there are some limitations for our current work.

Firstly, due to the nature of reverse-mode automatic differentiation, the memory cost is large because we need to save all the intermediate results. This poses a big challenge, especially when we use a fine grid for numerical simulation. One remedy is to consider distributed computing. For example, we can use MPI (message passing interface) techniques (Gropp et al. 1996) to scale the problem by utilizing multiple processors and computer nodes. This is under development for the ADCME library.

Secondly, optimization with deep neural networks leads to a nonconvex optimization problem. This poses a challenge for gradient-based optimization algorithms because local minima are inevitable. One approach is to impose some prior knowledge to the deep neural networks. For example, in 3.3 we considered a layered model for the viscosity coefficient. Although this does not solve the non-convex problem, we shrink the space of possible solutions and therefore make the inverse problem better conditioned.

Finally, it is difficult to determine whether the inverse problem is ill-posed before solving the inverse problem. That is, two different $\nu(\mathbf{x})$ may produce similar observations. We plan to develop diagnostic guidance for determining when the problem is ill-posed in our approach.

5 Conclusion

We have proposed a novel and general approach for solving inverse problems for the steady state Navier-Stokes equations. In particular, we consider estimating spatially-varying physical coefficients (e.g., viscosity and conductivity) in coupled systems from (partially observed) state variables. The key is to express the numerical simulation using a computational graph and implement the forward computation using operators (nodes in the computational graph) that can back-propagate gradients. Then, the gradients of the loss functions with respect to the unknown parameters can be extracted automatically. We approximate the unknown physical field using a deep neural network and calibrate its weights and biases using a gradient-based optimization approach. Computing the gradients requires back-propagating gradients through both numerical solvers and deep neural networks.

Our major finding is that the deep neural network provides regularization compared to pixel-wise approximations

in the case of small and indirect data (partially observed state variables). We demonstrate the effectiveness and wide applicability on three different inverse modeling problems that involve the Navier-Stokes equations. We implemented our approach in the following two libraries, which can be easily generalized and applied to other inverse problems:

1. ADCME.jl¹: automatic differentiation backend;
2. PoreFlow.jl²: a collection of numerical simulation operators.

Acknowledgement

This research was supported by U.S. Department of Energy, Office of Advanced Scientific Computing Research under the Collaboratory on Mathematics and Physics-Informed Learning Machines for Multiscale and Multiphysics Problems (PhILMs) project, PhILMS grant DE-SC0019453.

The authors want to acknowledge ANSYS, Inc. for support and Rishikesh Ranade, Haiyang He, Amir Maleki, Jan Heyse, and Wentai Zhang on the Chief Technology Officer team for helpful suggestions.

References

- [Basu et al. 2020] Basu, S.; Holbrook, L. T.; Kudlaty, K.; Fasanmade, O.; Wu, J.; Burke, A.; Langworthy, B. W.; Farzal, Z.; Mamdani, M.; Bennett, W. D.; et al. 2020. Numerical evaluation of spray position for improved nasal drug delivery. *Scientific reports* 10(1):1–18.
- [Baydin et al. 2017] Baydin, A. G.; Pearlmutter, B. A.; Radul, A. A.; and Siskind, J. M. 2017. Automatic differentiation in machine learning: a survey. *The Journal of Machine Learning Research* 18(1):5595–5637.
- [Beam and Bailey 1988] Beam, R. M., and Bailey, H. E. 1988. Newtons method for the navier-stokes equations. In *Computational Mechanics* 88. Springer. 1457–1460.
- [Cotter et al. 2009] Cotter, S. L.; Dashti, M.; Robinson, J. C.; and Stuart, A. M. 2009. Bayesian inverse problems for functions and applications to fluid mechanics. *Inverse problems* 25(11):115008.
- [Fedorov and Viskanta 2000] Fedorov, A. G., and Viskanta, R. 2000. Three-dimensional conjugate heat transfer in the microchannel heat sink for electronic packaging. *International Journal of Heat and Mass Transfer* 43(3):399–415.
- [Goodfellow et al. 2016] Goodfellow, I.; Bengio, Y.; Courville, A.; and Bengio, Y. 2016. *Deep learning*, volume 1. MIT press Cambridge.
- [Gropp et al. 1996] Gropp, W.; Lusk, E.; Doss, N.; and Skjellum, A. 1996. A high-performance, portable implementation of the mpi message passing interface standard. *Parallel computing* 22(6):789–828.
- [Li et al. 2020] Li, D.; Xu, K.; Harris, J. M.; and Darve, E. 2020. Coupled time-lapse full waveform inversion for sub-surface flow problems using intrusive automatic differentiation. *Water Resources Research* e2019WR027032.

¹<https://github.com/kailaix/ADCME.jl>

²<https://github.com/kailaix/PoreFlow.jl>

- [Liu and Nocedal 1989] Liu, D. C., and Nocedal, J. 1989. On the limited memory bfgs method for large scale optimization. *Mathematical programming* 45(1-3):503–528.
- [Margossian 2019] Margossian, C. C. 2019. A review of automatic differentiation and its efficient implementation. *Wiley Interdisciplinary Reviews: Data Mining and Knowledge Discovery* 9(4):e1305.
- [Rannacher 2000] Rannacher, R. 2000. Finite element methods for the incompressible navier-stokes equations. In *Fundamental directions in mathematical fluid mechanics*. Springer. 191–293.
- [Wang, Wang, and Li 2007] Wang, J.; Wang, M.; and Li, Z. 2007. A lattice boltzmann algorithm for fluid-solid conjugate heat transfer. *International journal of thermal sciences* 46(3):228–234.
- [Xu and Darve 2020] Xu, K., and Darve, E. 2020. Physics constrained learning for data-driven inverse modeling from sparse observations. *arXiv preprint arXiv:2002.10521*.
- [Zajaczkowski, Haupt, and Schmehl 2011] Zajaczkowski, F. J.; Haupt, S. E.; and Schmehl, K. J. 2011. A preliminary study of assimilating numerical weather prediction data into computational fluid dynamics models for wind prediction. *Journal of Wind Engineering and Industrial Aerodynamics* 99(4):320–329.